Dynamics of Polymer "Isotope" Mixtures: Molecular Dynamics Simulation and Rouse Model Analysis

A. Kopf*, B. Dünweg† and W. Paul*

Abstract

We report results of a molecular dynamics simulation of an "isotope" mixture of polymer chains, which are represented by a standard bead–spring model, and whose two species differ *only* by their monomer masses. Detailed analysis of the Rouse modes shows that for sufficiently short (non–entangled) chains this system can be well described by the Rouse model. Each species is described by its individual monomeric friction coefficient, whose dependence on both mass ratio as well as mixing ratio is studied. The main effect of mixing is an acceleration of the slower chains and a slowdown of the faster ones, while both species remain dynamically different. Some microscopic insight into the mechanism is obtained by studying the short–time behavior of the monomeric velocity autocorrelation function. Studies in the slightly entangled regime (chain length up to $N = 150$, where the typical entanglement chain length is $N_e \approx 35$) seem to further corroborate the hypothesis that the "tube diameter" of the reptation model is a quantity which results mainly from the *static* configurations, i. e. is an equilibrium thermal average. The usefulness of recently suggested analysis methods in this regime is briefly discussed.

PACS: 83.20.Jp, 83.10.Nn, 83.20.Fk, 83.80.Es, 61.25.Hq, 61.41.+e

---

*Institut für Physik, Johannes–Gutenberg–Universität, D–55099 Mainz, Germany

†Max–Planck–Institut für Polymerforschung, Ackermannweg 10, D–55128 Mainz, Germany

I. INTRODUCTION

Polymer blends possess a number of technical advantages compared to one–component materials, since they often combine desired properties of the single components. A particularly important feature is the possibility to vary the glass transition temperature of the blend via the mixing ratio. Due to this practical interest, the last few years have seen a number of investigations aiming at a deeper understanding of the dynamic processes in a compatible blend or a block copolymer melt in the homogeneous phase. In particular, the single–chain dynamics, which for a single–species melt is reasonably well understood in terms of the Rouse model for short–chain systems, or the reptation model for longer chains[1], is still rather unclear. The main difficulty is the complicated interplay of (i) the intrinsic viscoelastic melt behavior, (ii) onset of domain formation and critical composition fluctuations near the phase transition (which might however not be accessible due to the glass transition), and (iii) the mutual dynamic influence of the different components even far away from unmixing, which, as pure species, can have rather different dynamical properties. Recent studies have included scattering experiments[2,3], analytical theory[4–6] as well as computer simulations on a lattice[7]. Nevertheless a comprehensive and well–established theoretical framework for these processes is still lacking. This is in marked contrast to the status of the theories (and simulations[8]) of Rouse / reptation dynamics in melts[1,9–11], of the static phase behavior of blends and block copolymers[9,12–15], as well as the dynamics of collective composition fluctuations[13].

In order to cleanly separate the effects from each other, one would like to study a mixed system whose species differ *only* by their dynamic properties, but not by their static ones. This is extremely difficult to do in an experiment, since in a mixture there are always some chemical interactions which usually drive unmixing — even a mixture of protonated and deuterated (while otherwise identical) polymers has been shown to unmix[16] — such that there is hardly any situation in which the processes mentioned in (ii) can be neglected. Conversely, in a computer simulation it is rather easy to implement a model which comprises

a system of identical chains, which however are split up into species A ("fast chains") and species B ("slow chains"). There are several possibilities to do this. In a Monte Carlo model, one would assign different jump rates to the different species, while in a Brownian dynamics simulation the different species would be characterized by different monomeric friction coefficients. In a stochastic dynamics simulation one could choose different friction coefficients and/or masses, while in a microcanonical Molecular Dynamics (MD) simulation the only possibility is an assignment of different monomer masses. In the present study, we chose the last approach. For dense systems, both MD as well as stochastic dynamics are computationally quite efficient, but MD has the additional advantage of reproducing the overall momentum conservation, which is important for the hydrodynamic properties[17]. The closest experimental system to this model would be a mixture of chains which are identical except for the nuclear masses (isotope mixture). However, in the computer model we varied the monomer mass ratio up to the value 100 (which is not accessible experimentally). Moreover, an experimental isotope mixture would exhibit some residual differences in the chemical interaction, while the interactions in the computer model are strictly identical. Hence the system is best viewed as a particularly simple model designed to study the mutual dynamic influence of slow and fast chains onto each other.

We have only been able to do this study in the chain length regime where the corresponding single–species system exhibits Rouse–like behavior. It is the purpose of the present paper to demonstrate that the mixed system can be well described by the Rouse model, too. However, the different species must be described by different monomeric friction coefficients. In the regime of longer chains the present study has faced the usual prohibitive computational demands which occur when one tries to probe the system well above the entanglement threshold[10,18]. Hence, only qualitative results on the dynamics of entangled mixtures have been obtained. For instance, our simulation results indicate that the "tube diameter" of reptation theory[1] is a *static* quantity (equilibrium thermal average).

We have studied exactly the same model as the one simulated by Kremer and Grest[10] for the single–species case. Hence, all the relevant static properties, as well as the order

of magnitude of relaxation times etc., were already known beforehand. In particular, this knowledge could be used for an efficient equilibration procedure. Details of the model and technical details are described in Sec. II, and some static quantities (which of course coincide with those in Ref. 10) are reported in Sec. III. Sec. IV reports on our results for the dynamics, which are elucidated in more detail in Sec. V, which describes the analysis in terms of Rouse modes. Sec. VI presents results on slightly entangled chains, and Sec. VII concludes with a summary and discussion.

II. MODEL AND SIMULATION TECHNIQUE

The bead–spring polymer melt model studied by Kremer and Grest[10] consists of M chains of N monomers each. The excluded volume interaction is modeled via a purely repulsive Lennard–Jones potential acting between all monomers,

$$U_{LJ}(r) = \begin{cases} 4\varepsilon \left[\left(\frac{\sigma}{r}\right)^{12} - \left(\frac{\sigma}{r}\right)^{6} + \frac{1}{4} \right] & r \le 2^{1/6}\sigma \\ 0 & r \ge 2^{1/6}\sigma, \end{cases} \tag{2.1}$$

where r is the distance between the monomers, and the energy parameter ε as well as the length parameter σ are set equal to unity in order to fix energy and length units. Consecutive monomers along a chain are connected via the FENE potential

$$U_{ch}(r) = -\frac{k}{2} R_0^2 \ln\left(1 - \frac{r^2}{R_0^2}\right), \tag{2.2}$$

where $R_0 = 1.5$ is the maximum extension of the nonlinear spring, and $k = 30$ is the spring constant. These parameters had been optimized in order to assure non–crossing of the chains at the simulated density $\rho = 0.85$, as well as reasonable match of the oscillation times associated with the two potentials[19]. The temperature was chosen as $k_B T = 1$, and the simulation was run in a cubic box with periodic boundary conditions.

As the potentials do not depend on the velocities, the momenta are, in the canonical ensemble, strictly statistically independent of the coordinates, and their probability distribution is simply the Maxwellian distribution. Therefore, the masses are only important for

those static quantities which depend on the momenta (like the mean square velocity of a monomer, for instance). On the other hand, the problem of equilibrating the polymer melt is, in practice, identical to the equilibration of the configurational degrees of freedom (the momenta relax much faster). Therefore, we first generated well–equilibrated configurations of the polymer melt using the following procedure from Kremer and Grest[10]: From the previous simulations[10] the mean square bond length is known rather accurately,

$$\left\langle b^2 \right\rangle = \left\langle (\vec{r}_{i+1} - \vec{r}_i)^2 \right\rangle = 0.94, \tag{2.3}$$

i and $i+1$ being consecutive monomers along a chain. Similarly the stiffness parameter C_∞, defined via a chain's mean square end–to–end distance

$$\left\langle R^2(N) \right\rangle = \left\langle (\vec{r}_N - \vec{r}_1)^2 \right\rangle = C_\infty \left\langle b^2 \right\rangle (N-1)\,, \tag{2.4}$$

has the known value $C_\infty = 1.74$ (note that the excluded volume interaction is screened in the dense melt, and the chain statistics is Gaussian). Therefore, we generated for each chain a "non–reversal random walk" in the continuum, using the following procedure: Each monomer was added with a fixed bond length $b = \sqrt{\langle b^2 \rangle}$, and each new bond was allowed to rotate freely, except for the condition $|\vec{r}_i - \vec{r}_{i-2}| > d$, which takes into account the excluded volume interaction with the next nearest neighbor along the chain. Hence these random walks have the desired bond length, and, by adjusting the minimum distance d as

$$d = 2b\sqrt{\frac{C_\infty - 1}{C_\infty + 1}}, \tag{2.5}$$

also the correct stiffness parameter. Consequently the chains already have the desired global structure; however, the monomers will of course strongly overlap. In order to equilibrate also the local packing we then ran a simulation in which the connectivity potential as well as the excluded volume interaction between consecutive monomers were fully established, while the repulsive Lennard–Jones potential between non–consecutive monomers was replaced by a much softer potential,

$$U_c(r) = \begin{cases} A\left[1 + \cos\left(\pi r / 2^{1/6}\sigma\right)\right] & r \le 2^{1/6}\sigma \\ 0 & r \ge 2^{1/6}\sigma, \end{cases} \tag{2.6}$$

whose strength parameter A was slowly increased from $A = 1$ to $A = 60$. For these equilibration runs we used stochastic dynamics, i. e. Molecular Dynamics augmented with a frictional force and a Langevin noise term[19,20]:

$$m\frac{d^2\vec{r}_i}{dt^2} = -\frac{\partial U}{\partial \vec{r}_i} - \Gamma\frac{d\vec{r}_i}{dt} + \vec{W}_i(t), \tag{2.7}$$

where the stochastic forces $\vec{W}_i(t)$ on the i–th monomer and the friction constant Γ are related to each other by the fluctuation–dissipation theorem

$$\langle \vec{W}_i(t) \cdot \vec{W}_j(t') \rangle = \delta_{ij}\delta(t-t')6k_BT\,\Gamma. \tag{2.8}$$

Since these runs had the sole purpose of equilibrating the configurational degrees of freedom, we assigned the same mass to all monomers (any other choice of masses would have resulted in a slower relaxation into equilibrium). Setting this mass m equal to unity fixes the mass and time units, i. e. time is measured in units of $\tau = (m\sigma^2/\varepsilon)^{1/2}$. For the monomeric friction constant we chose the standard value[10] $\Gamma = 0.5$, which corresponds to a rather weak coupling, i. e. a dynamics which is similar to the strictly microcanonical case ($\Gamma = 0$). The velocity Verlet algorithm was applied, using a time step of $h = 3 \times 10^{-3}$. First, A was increased every 120 MD steps by $\Delta A = 5$ until $A = 60$ was reached. Note that the increase of A should not be done too slowly — otherwise the chains would feel a thermodynamic driving force towards a smaller C_∞ for a too long time, and hence temporarily decrease their size from the initial optimum value. Then we ran the system with $A = 60$ for an additional equilibration time of roughly 3×10^4 MD steps. After that, we replaced the soft potential by the full repulsive interaction according to Eqn. 2.1, and a further equilibration was added for at least another 5×10^5 MD steps.

After equilibration, we started to study systems with different masses. We randomly selected xM chains, $x < 1$, out of the M chains in total, and assigned a larger mass $m_s > m = m_f$ to each of their monomers. Each monomer was assigned a new random velocity, generated from the correct Maxwellian distributions corresponding to the new masses. From then on, the system was run purely microcanonically, using the velocity Verlet algorithm

with a time step $h = 3 \times 10^{-3}$. Time units are fixed by the convention that the monomer mass of the *light* component is set to unity. Tests showed that this choice ensures stability for very long runs with several million time steps. For example, for a run with a total length of 56×10^6 MD steps the fractional energy drift was only $(E(t) - E(0))/E_{kin} = .53\%$. All results were averaged over 10 independent runs.

In order to save computer time, we implemented a multiple time step scheme along the lines suggested by Tuckerman *et al.*[21], which updates the slower degrees of freedom less frequently. However, for our system the approach turned out to yield significant gains only for the most extreme cases, i. e. the largest mass ratio ($m_s/m_f = 100$), and rather large fractions of slow chains. We also introduced a slight modification, which ensures strict total momentum conservation. The details of this algorithm are presented elsewhere[22]. Most simulations were run on a Convex/HP SPP 1000 and a Convex/HP SPP 1200 with PA-7000 and PA-7200 RISC–processors, respectively. Using a scalar version of a link cell scheme combined with a Verlet table[23], our program attained a performance of 1.3×10^5 particle updates (MD steps times number of monomers) per second per processor.

Note that the case $x = 0$ (all chains fast) is precisely the system studied by Kremer and Grest[10]. Moreover, the case $x = 1$ (all chains slow) can be trivially deduced from the data for $x = 0$ by a simple rescaling of time, as is immediately seen via the identity

$$m\frac{d}{dt^2} = \frac{d}{d\left(t/\sqrt{m}\right)^2}. \tag{2.9}$$

The mass ratio was chosen as $m_s/m_f = 2, 4$, and 100, implying a ratio of the natural time scales of $\tau_s/\tau_f = 1.41, 2$, and 10. Table I gives an overview over the simulated systems.

III. STATIC PROPERTIES

We calculated some static quantities like pressure, mean square end–to–end distance (Eqn. 2.4), mean square gyration radius

$$\left\langle R_G^2 \right\rangle = N^{-1} \sum_{n=1}^{N} \left\langle (\vec{r}_n - \vec{r}_{CM})^2 \right\rangle \tag{3.1}$$

($\vec{r}_{CM}$ denoting the chain's center of mass), and the single–chain static structure factor

$$S(\vec{q}) = \frac{1}{N} \left\langle \left| \sum_{n=1}^{N} \exp\left(i\vec{q} \cdot \vec{r}_n\right) \right|^2 \right\rangle . \tag{3.2}$$

Within statistical accuracy, our data coincide with those reported by Kremer and Grest[10]. The pressure decreases with increasing degree of polymerization (see Table I), due to the decreasing density of chain ends. The chains obey Gaussian statistics, as expected for a dense melt and revealed via the behavior $\langle R^2 \rangle \propto N - 1$, $\langle R_G^2 \rangle \propto N - 1$, and the fractal scattering law[24] $S(q) \propto q^{-2}$ for $R_G^{-1} \ll q \ll b$ (data not shown).

Moreover, we found precisely the same static single–chain properties for both the fast and slow chains, as it should be. This is an important check on our ability to calculate meaningful averages also for the slow chains, up to a mass ratio $m_s/m_f = 100$.

IV. DYNAMIC PROPERTIES

In contrast to the statics, the dynamic properties will show a clear dependence on the monomer masses. Before discussing the situation in a mixture we look at a pure system with all masses equal to unity. Again, this case is exactly the model studied in Ref. 10, and our results are well consistent with the older data. However, the dynamics turned out to be a few percent faster for our runs than for those of Ref. 10. We ascribe this difference to the difference between the stochastic dynamics used in Ref. 10 and the microcanonical algorithm used in the present study.

The standard picture on the dynamics of single–component melts[1,25] can be briefly summarized as follows: Melts of extremely short chains (say, $N < 10$) are best viewed as simple liquids — these chains are simply too short for any scaling behavior (like the Gaussian statistics of the chain conformations) to be observable. Melts of longer chains can then be reasonably described by the Rouse model[1], which simply assumes that a test chain moves in the same way as a random walk would move whose monomers are coupled to a homogeneous viscous background. The model lumps together all the complicated matrix effects into one

single parameter, the monomeric friction constant ζ. For our model, Kremer and Grest[10] found that the crossover to reptation sets in rather early, and hence the effective ζ increases systematically with chain length from $\zeta \approx 15$ for very short chains ($N = 5$) to $\zeta \approx 25$ for the longest chains ($N = 200$).

Since the monomer motion in the Rouse model is described as pure Brownian motion, it is of course only valid on time scales on which the influence of deterministic short–time motion is no longer observed. This defines a "microscopic" time scale τ_b, beyond which the validity of the Rouse model sets in, and which roughly corresponds to the time which is needed for the monomer to move a bond length b. Similarly, the longest relaxation time, the Rouse time τ_R, corresponds to the motion of the chain as a whole over a distance of order R_G. The behavior on intermediate length and time scales then follows from simple dynamic scaling. As simulations[10,11] have shown for several models, this simple concept works surprisingly well. However, the Rouse description holds only for chain lengths which are not too high. For larger chains, the effects of the temporary constraints (i. e. the non–crossability) can no longer be accounted for by a homogeneous background. Reptation theory[1] is the most successful (however not undisputed[26,27]) theoretical picture so far, taking these effects approximately into account. In this theory, the chain is viewed as being constrained in a temporary tube, which forces it to move predominantly along its own contour. Therefore, there is an additional length scale involved, the tube diameter d_T, which is mapped via $d_T^2 \propto \langle R_G^2(N_e)\rangle$ onto the entanglement chain length N_e. The older simulations[10] have shown that for the present model in the homogeneous case $N_e \approx 35$. Melts with $N \gg N_e$ must be viewed as highly entangled; however, limitations in computer speed have made it impossible so far to go deeply into this regime. It should be noted that the concept of a characteristic chain length N_e, above which slowing down compared to Rouse behavior sets in, is also present in other theoretical approaches which have been developed as alternatives to[26,27] or generalizations of[28] standard reptation theory[1], and also observed in neutron spin echo experiments[29–31].

The current and the subsequent section will be devoted to the Rouse regime, and hence

we will limit ourselves to rather short chain lengths. Most data will be presented for $N = 20$ or $N = 30$; we view these chains as sufficiently long to exhibit random walk behavior reasonably well, while being still far away from the entangled regime. In the Rouse model, the center–of–mass diffusion constant is proportional to N^{-1}, $D = (k_B T)/(\zeta N)$. The overall chain moves diffusively, i. e. for time scales $t \gg \tau_b$

$$g_3(t) \equiv \left\langle [\vec{r}_{CM}(t) - \vec{r}_{CM}(0)]^2 \right\rangle \propto t. \tag{4.1}$$

However, nearly all polymer simulations[10,11], including ours, show a slightly different behavior: While indeed for large times $t \gg \tau_R$ simple diffusion ($g_3 \propto t^1$) takes place, the data for $\tau_b \ll t \ll \tau_R$ are better described via $g_3 \propto t^{0.8}$. This observation is so far not fully understood; since this power law is not found in single–chain simulations in a frozen medium it is very likely a many–chain effect[25]. Apart from g_3, the dynamics is commonly studied in terms of the mean square displacement of a single monomer (located at the center of the chain, in order to minimize end effects), both in the "laboratory system",

$$g_1(t) \equiv \left\langle \left[\vec{r}_{N/2}(t) - \vec{r}_{N/2}(0)\right]^2 \right\rangle, \tag{4.2}$$

as well as in the chain's center–of–mass system,

$$g_2(t) \equiv \left\langle \left[\vec{r}_{N/2}(t) - \vec{r}_{CM}(t) - \left(\vec{r}_{N/2}(0) - \vec{r}_{CM}(0)\right)\right]^2 \right\rangle. \tag{4.3}$$

For long times $t \gg \tau_R$, the overall diffusion takes over, i. e. $g_1 \approx g_3 \propto t$, while g_2 saturates at a constant value proportional to R_G^2. On the intermediate time scales $\tau_b \ll t \ll \tau_R$, dynamic scaling implies (omitting prefactors of order unity)

$$g_1(t) \approx g_2(t) \approx R_G^2 \left(\frac{t}{\tau_R}\right)^{1/2} \tag{4.4}$$

(note $\tau_R \propto N^2 \propto R_G^4$). Of course, for extremely short times all three displacements are proportional to t^2, due to the underlying Newtonian dynamics. Figs. 1 and 2 show $g_1(t)$ and $g_3(t)$ for a pure system for various chain lengths. We find that our simulation reproduces Rouse behavior quite satisfactorily up to chain length $N = 30$, while for $N = 50$ already a slight slowing down is observable.

Let us now discuss the same quantities for mixed systems. Fig. 3 studies the motion of the light chains for chain length $N = 30$, for both the pure system as well as two 50% mixtures (mass ratio $m_s/m_f = 4$ and 100). If there were no matrix effects, the curves would coincide. However, as is seen from both g_1 as well as g_3, the light chains get slowed down substantially upon increasing the mass of the heavier chains. The slopes of the curves indicate that the chains should be still describable by the Rouse model, but the monomeric friction coefficient is significantly increased due to the matrix effect. A quantitative analysis of this picture is done in Sec. V.

The reverse effect is observed for the heavy chains: In Fig. 4 we plot g_1 and g_3 for the heavy chains, and the same system as before. In order to remove the trivial slowing down induced by the larger mass, the displacements are shown as a function of scaled time $t\sqrt{m_f/m_s}$. This is equivalent to keeping the mass of the heavy chains fixed, while decreasing the mass of the light chains, such that again the curves would coincide in the absence of matrix effects. As is seen from the figure, the heavy chains get the faster the lighter the other component gets. Again the typical Rouse power laws are observable, i. e. also the slow chains are describable by the Rouse model, choosing a suitable friction coefficient.

Moreover, we observe that the matrix effects on a test chain get more and more pronounced when the fraction of the other component is increased: Fig. 5 shows g_1 and g_3 of the light chains for a fixed mass ratio $m_s/m_f = 4$, but varying mixing ratio (chain length $N = 20$). Again the fastest dynamics is found in the pure system. The higher the fraction of heavy particles is the slower the light polymers become. Finally, we find that in the mixed system the originally faster chains are still somewhat faster than the slow ones.

Note that from a simple Stokes–Einstein picture (which works quite well for simple single–species liquids, see, e. g., Ref. 32) one would have expected that the monomeric friction coefficient would only depend on the effective monomer size, which is of course the same for both species, and on the viscosity, which is of course affected by mass and mixing ratio (large mass means slow stress relaxation), but also a global property of the overall system. Hence, from simple Stokes–Einstein arguments one would have expected a

polymer dynamics which is *independent* of the species. Hence, the results show clearly that the monomer friction coefficient is in our case a more complex quantity which cannot be determined reliably from simple hydrodynamics.

After having established that the matrix effects can be described by an effective *microscopic* parameter ζ, one can hope to gain some more insight by looking at the phenomena on a more microscopic time and length scale. To this end, we study the normalized velocity autocorrelation function

$$\frac{\langle \vec{v}(t) \cdot \vec{v}(0) \rangle}{\langle \vec{v}^2 \rangle} \tag{4.5}$$

of a monomer, which of course contains precisely the same dynamic information as the mean square displacement, but visually exhibits more structure on short time scales.

Fig. 6 displays this function for a pure system. For comparison with data for mixed systems, we rescaled time such that Fig. 6 is effectively plotted for a pure system with monomer mass $m = 4$. The different curves correspond to different monomer indices such that end effects are visible. Within the accuracy of the simulation, we observe that the velocity autocorrelation function is the same for all monomers, except those at the very ends of the chain. Moreover, comparing Fig. 6 with typical velocity autocorrelation functions for dense simple liquids[33], one immediately notices the big number of oscillations, originating in the vibrations along the backbone of the chain. Since the end monomers have got only one neighboring monomer they couple less strongly to the backbone oscillations resulting in a less pronounced first peak.

Another interesting observation is a quite well–defined separation of time scales. After two oscillations the function has decayed already rather strongly, while it afterwards exhibits a very long but weak negative tail. This is again a reflection of Rouse–like dynamics: Ignoring the tail, one would obtain a quite large integral, which would correspond to a short–time diffusion constant, or, via the Einstein relation, to the monomeric friction coefficient ζ. In contrast, upon integrating the full autocorrelation function, one obtains the true long–time diffusion constant, which is of course the much smaller diffusion constant of the overall

chain. Nevertheless, this separation of time scales is somewhat ambiguous and hence not particularly useful for the determination of ζ. A more reliable quantitative procedure rests on the long–time behavior and exploitation of the Rouse scaling $\tau_R \propto N^2$, which will be done in Sec. V.

We now focus upon the velocity autocorrelation function of middle monomers for mixed systems (of chain length $N = 20$), where we keep the mass ratio $m_s/m_f = 4$ fixed, and vary the composition. This is shown in Fig. 7 for the heavy monomers. One sees that the *frequencies* of the oscillations depend only extremely weakly on the mixing ratio, while the *amplitudes* show a significant effect. This indicates that the oscillations are indeed mainly due to the coupling to the neighbors along the chain, while the effect of the matrix is mainly an average damping due to the "random collisions" with other monomers. As is clearly seen from Fig. 7 (and the analogous data for light monomers), the motion of both the heavy monomers as well as of the light monomers gets more and more efficiently damped upon increasing the fraction of the heavy component: Heavy monomers absorb momentum more efficiently than light ones. Thus the observed matrix effects on the monomeric friction coefficient can, to a certain extent, be traced back to the collisional kinematics between monomers of various masses. The microscopic origin is clearly the short–time dynamics.

V. ROUSE MODE ANALYSIS

This section is devoted to the quantitative determination of the monomeric friction coefficient ζ for each species. To this end, we start from the known exact solution of the Rouse model for Gaussian chains[34,1]. The effective Hamiltonian (in three spatial dimensions), which describes the Gaussian statistics of the chain, is

$$\mathcal{H} = \frac{3k_BT}{2b^2} \sum_{i=1}^{N-1} \left(\vec{r}_{i+1} - \vec{r}_i\right)^2 , \tag{5.1}$$

where b^2 is the mean square bond length. This results in the Langevin equation for the ith monomer

$$\frac{d}{dt}\vec{r}_i = -\frac{1}{\zeta}\frac{\partial \mathcal{H}}{\partial \vec{r}_i} + \vec{\rho}_i, \tag{5.2}$$

where the mean square stochastic displacements are related to the temperature via the fluctuation–dissipation theorem,

$$\langle \vec{\rho}_i(t) \cdot \vec{\rho}_j(t') \rangle = \delta_{ij} 6(k_B T/\zeta)\delta(t-t'). \tag{5.3}$$

The orthogonal transformation from monomer coordinates $\vec{r}_i$ to Rouse modes $\vec{X}_p$, $p = 0, 1, \ldots, N-1$, via

$$\vec{X}_0 = N^{-1/2} \sum_{i=1}^{N} \vec{r}_i \tag{5.4}$$

$$\vec{X}_p = \sqrt{2}\, N^{-1/2} \sum_{i=1}^{N} \vec{r}_i \cos\left[\frac{p\pi}{N}\,(i-1/2)\right] \qquad p \geq 1$$

(which is identical to the definition given in Ref. 35) decouples the equations of motions, such that each Rouse mode can be viewed as a coordinate which performs a Brownian motion in a harmonic potential, independently of all others[1]. Hence, for $p \geq 1$,

$$\left\langle \vec{X}_p(t) \cdot \vec{X}_p(0) \right\rangle = \left\langle \vec{X}_p^2 \right\rangle \exp\left(-t/\tau_p\right) \tag{5.5}$$

with

$$\left\langle \vec{X}_p^2 \right\rangle = \frac{b^2}{4\sin^2\left(\frac{p\pi}{2N}\right)} \tag{5.6}$$

and

$$\tau_p^{-1} = \frac{12 k_B T}{\zeta b^2} \sin^2\left(\frac{p\pi}{2N}\right). \tag{5.7}$$

It should be noted that in the literature sometimes other definitions of Rouse modes are given[25]. However, we have carefully checked the transformation and convinced ourselves that the one given by Eqn. 5.4 is the correct one. Nevertheless, we also found that the difference is only of minor practical importance, since numerically it amounts to at most a few percent in the relaxation rates.

The data analysis then proceeds by calculating $\vec{X}_p$ from the monomer coordinates via Eqn. 5.4, and calculating the mode autocorrelation function, which is then compared with Eqn. 5.5. Since the mean square bond length b^2 is known as a static average, the relaxation rate allows us to extract ζ from Eqn. 5.7. In practice, we considered only the first four Rouse modes $1 \leq p \leq 4$, since for higher modes the deviations from Gaussian statistics were already too severe, given the rather short chain lengths which we considered.

For a pure system ($N = 30$) the decay of $\left\langle \vec{X}_p(t) \cdot \vec{X}_p(0) \right\rangle$, as a function of scaled time $t \sin^2\left(\frac{p\pi}{2N}\right)$, is shown in Fig. 8 for $1 \leq p \leq 4$. In Table II data for ζ are shown, as obtained for $N = 10$, 20, 30, and $1 \leq p \leq 4$. It seems that the mode $p = 1$ yields a slightly lower value for ζ than the higher modes. This might be due to some slight deviations from ideal Rouse behavior; however, our numerical accuracy is not sufficient to prove this unambiguously.

For the mixed systems, we first checked if modes with different mode index $p \neq q$ are uncorrelated for all times; within our error bars, they are (any other result would have been quite surprising). Then we proceeded with the same analysis of the relaxation rates as for the pure system, for each species separately. For example, Fig. 9 shows the first four modes of the heavy polymer species plotted as a function of scaled time in a blend with mass ratio $m_s/m_f = 100$ and 20% light chains. Taking into account the somewhat worse statistics (the heavy chains have a longer relaxation time, and only 80% of the system contribute to the mode autocorrelation function), and comparing with Fig. 8, we conclude that the Rouse model has the same validity in the mixture as in the pure system. By using two different phenomenological monomer friction coefficients one is able to describe the dynamics of both polymer species in the blend.

The friction coefficients which we thus obtained (for the mode $p = 1$) are shown for chain lengths $N = 20$ and $N = 30$ and mass ratios $m_s/m_f = 2, 4, 100$ in Fig. 10. These data sum up the discussed increase of both friction coefficients as a function of both x (fraction of heavy polymers) as well as m_s. Within our accuracy, no systematic dependence of ζ on the chain length N could be observed in the range $10 \leq N \leq 30$.

VI. CROSSOVER TO REPTATION BEHAVIOR

The reptation picture for long chains, $N \gg N_e$, involves four relevant time scales, the microscopic time τ_b, the entanglement time $\tau_e \propto N_e^2$, the Rouse time $\tau_R \propto N^2$, and the disengagement time $\tau_d \propto N^3/N_e$. The reptation model predicts a sequence of crossovers

$$g_1(t) \propto \begin{cases} t^{1/2} & \tau_b \ll t \ll \tau_e \\ t^{1/4} & \tau_e \ll t \ll \tau_R \\ t^{1/2} & \tau_R \ll t \ll \tau_d \\ t^1 & \tau_d \ll t. \end{cases} \tag{6.1}$$

A similar behavior is predicted for g_2 (except for a final t^0 behavior, of course), while g_3 should behave like

$$g_3(t) \propto \begin{cases} t^1 & \tau_b \ll t \ll \tau_e \\ t^{1/2} & \tau_e \ll t \ll \tau_R \\ t^1 & \tau_R \ll t. \end{cases} \tag{6.2}$$

For more details on the theory, see Ref. 1. A recent overview over the various difficulties to observe reptation behavior in computer simulations is given in Ref. 18. The main problem is the necessity to study long chains $N \gg N_e$, while on the other hand in this limit the longest relaxation time, $\tau_d \propto N^3$, gets prohibitively large. The clearest indication of reptation–like behavior is usually the crossover in g_1 from $t^{1/2}$ to $t^{1/4}$. Nevertheless, no simulation has so far been able to observe this latter power law clearly; rather the observed exponents are always larger than 0.25. The explanation of this, in the reptation picture, is the too close proximity of the two adjacent $t^{1/2}$ regimes, which, due to smooth crossovers, blur the $t^{1/4}$ behavior. Our simulation data have little to add to change this unfortunate state of affairs. However, if one accepts the reptation scenario as such, one can extract the best estimate for τ_e via power–law fits to the two regimes. This, in turn, allows an estimate of the "tube diameter" d_T via $g_1(\tau_e) = d_T^2$. This can be done reasonably well for the longest chains we have studied, $N = 150$. Instead of a well–defined change from $t^{1/2}$ to $t^{1/4}$ we observe effective

exponents 0.46 and 0.37, while $d_T^2 \approx 20$. Beyond the framework of the reptation picture, d_T can at any rate be viewed as a characteristic length for slowing down, as it is also present in alternative pictures[26,27], which however predict different power laws.

An interesting question then is whether d_T should be viewed as a static quantity (i. e. an equilibrium configurational average like, e. g., $\langle R_G^2 \rangle$, which is in accord with the intuitive picture of topological constraints), or as a purely dynamic quantity (note that a determination of d_T has so far only been possible by studying the dynamics). In the first case, d_T would not depend on the details of the dynamics, and would be the same for all mass and mixing ratios. Conversely, in the "dynamic" case d_T would depend on the behavior of dynamic correlation functions and hence on the details of the dynamics; i. e. in this case one should expect some dependence on mass and mixing ratio. In order to answer this question, we took the data for a pure system as well as those for a 50% mixture (mass ratio $m_s/m_f = 100$, chain length always $N = 150$) and rescaled time for each data set such that the data fall on top of each other for times $t < \tau_e$. In this time regime, pure Rouse dynamics should apply, and hence such a rescaling is possible — this was the result of the previous sections. If each sort of chain had a different d_T, then the curves should splay after τ_e. However, within the accuracy of our data they do not, see Fig. 11, and this implies that the tube diameter is independent of the monomeric mass found in the system. Therefore we conclude that the tube diameter (or, beyond the reptation picture, the characteristic length scale of slowing down) is a static quantity or that its dependence on the details of the dynamics must be quite weak. This result further supports the reptation picture based upon topological foundations, and yields a further criterion for theories of polymer dynamics which they should satisfy.

Recently Ebert *et al.*[36] suggested to study also higher moments of the displacements, like

$$g^{(4)}(t) \equiv \langle \sum_{\mu=x,y,z} \left(r^{\mu}_{N/2}(t) - r^{\mu}_{N/2}(0) \right)^4 \rangle^{1/2}. \tag{6.3}$$

Analysis of $g^{(4)}$ should give clearer signs of reptation, and furthermore the crossover to reptation behavior should be observable at a shorter time. We hence tested these ideas for our system.

Firstly, we would like to point out that $g^{(4)}$ cannot give any new information as long as pure Rouse dynamics applies: From the picture of Brownian motion in a harmonic potential, which is the motion of the $\vec{X}_p$, it is clear that $\vec{X}_p$ is a Gaussian variable[1]. Hence, $\vec{r}_i(t) - \vec{r}_i(0)$ can be expressed as linear combination of Gaussian variables, i. e. it is itself Gaussian. However, for a Gaussian distribution the higher moments are all trivially related to the second one; in particular, the fourth moment is just three times the square of the second moment. Hence, by exploiting the spatial isotropy, one finds $g^{(4)2} = g_1^2$ or $g^{(4)} = g_1$ (in other spatial dimensions one would obtain only proportionality). Hence, an earlier crossover to slowed down motion can hardly be expected, since at least for the short times (Rouse behavior) g_1 and $g^{(4)}$ must coincide. Indeed, Fig. 12 shows for our pure $N = 150$ system that also beyond $t = \tau_e$ the curves are practically indistinguishable. Hence, our data show that the analysis of higher moments does not give any further insight into the reptation problem and is not of practical usefulness, at least up the chain lengths we were able to simulate. The behavior observed by Ebert *et al.* seems to be an artifact of their hair–pin model.

VII. DISCUSSION AND OUTLOOK

The present study has clearly shown that the Rouse model provides a very useful description for our system. Both types of chains relax in a Rouse–like way, however, the fast chains are slowed down in the slow matrix, while the slow chains are accelerated in the fast matrix. Nevertheless, there remains a clear distinction in the relaxation rates. Attempts to estimate the viscosity for our system are currently under way, mainly in order to assess the implied deviations in ζ from Stokes–Einstein behavior more quantitatively. Since we were not able to go deeply into the entangled regime, we can however not exclude the possibility that a mixture of extremely long (highly entangled) chains of different species (but very similar statics) might exhibit nearly identical diffusion constants for both species, due to an "average matrix" effect.

We expect that real polymer blends sufficiently far away from the unmixing transition (where the effect of the interaction is weak) would show rather similar behavior as our system. Experiments on binary blends should be analyzed in terms of *two* Rouse relaxation rates. Apart from these considerations, the system is also ideally suited to study interdiffusion in polymer blends[13] via investigating collective equilibrium composition fluctuations. Studies along these lines are currently under way.

Of course, the present model is only the simplest one for dynamics in polymer mixtures. Substantially more complicated and interesting behavior is to be expected when going from the noninteracting case to a melt which actually shows a tendency for unmixing via an attractive interaction, or, similarly, to a melt whose chains have different static properties like different chain stiffnesses or different chain lengths. Nevertheless, we hope that the present study stimulates further investigations, both experimental as well as theoretical. We feel that the difference in dynamics on the monomeric level is an important feature in polymer blend dynamics, and should be accounted for in any theoretical approach.

ACKNOWLEDGMENTS

We thank K. Binder and K. Kremer fur useful discussions. A. K. acknowledges support by the German federal department for education and research (BMBF) under Grant No. 03–BI4MAI–7.

REFERENCES

[1] M. Doi and S. F. Edwards, *The Theory of Polymer Dynamics* (Clarendon Press, Oxford, 1986).

[2] G. Fytas, G. Meier, and D. Richter, J. Chem. Phys. **105**, 1208 (1996).

[3] B. Ewen, D. Richter, B. Farago, and U. Maschke, Progr. Colloid Polym. Sci. **91**, 121 (1993).

[4] U. Genz and T. A. Vilgis, J. Chem. Phys. **101**, 7101 (1994).

[5] U. Genz and T. A. Vilgis, J. Chem. Phys. **101**, 7111 (1994).

[6] T. A. Vilgis and G. Meier, J. Phys. I France **4**, 985 (1994).

[7] M. Müller and K. Binder, J. Phys. II France **6**, 187 (1996).

[8] *Monte Carlo and Molecular Dynamics Simulations in Polymer Science*, edited by K. Binder (Oxford University Press, New York, 1995).

[9] P. G. de Gennes, *Scaling Concepts in Polymer Physics* (Cornell University Press, Ithaca, 1979).

[10] K. Kremer and G. S. Grest, J. Chem. Phys. **92**, 5057 (1990).

[11] W. Paul, K. Binder, D. W. Heermann, and K. Kremer, J. Chem. Phys. **95**, 7726 (1991).

[12] P. J. Flory, *Principles of Polymer Chemistry* (Cornell University Press, Ithaca, 1953).

[13] K. Binder, Adv. Polym. Sci. **112**, 181 (1994).

[14] M. Müller and K. Binder, Macromolecules **28**, 1825 (1995).

[15] G. S. Grest, M.-D. Lacasse, K. Kremer, and A. M. Gupta, J. Chem. Phys. **105**, 10583 (1996).

[16] F. S. Bates and P. Wiltzius, J. Chem. Phys. **91**, 3258 (1989).

[17] B. Dünweg, J. Chem. Phys. **99**, 6977 (1993).

[18] B. Dünweg, G. S. Grest, and K. Kremer, 1997, to appear, conf. proceedings, IMA workshop May 1996, Univ. Minn.

[19] G. S. Grest and K. Kremer, Phys. Rev. A **33**, 3628 (1986).

[20] T. Schneider and E. Stoll, Phys. Rev. **B 17**, 1302 (1978).

[21] M. E. Tuckerman, B. J. Berne, and G. J. Martyna, J. Chem. Phys. **97**, 1990 (1992).

[22] A. Kopf, W. Paul, and B. Dünweg, Comp. Phys. Comm. **101**, 1 (1997).

[23] G. S. Grest, B. Dünweg, and K. Kremer, Comp. Phys. Comm. **55**, 269 (1989).

[24] J. S. Higgins and H. C. Benoit, *Polymers and Neutron Scattering* (Clarendon Press, Oxford, 1994).

[25] K. Kremer and G. S. Grest, in 8.

[26] K. S. Schweizer, J. Chem. Phys. **91**, 5802 (1989).

[27] K. S. Schweizer, J. Chem. Phys. **91**, 5822 (1989).

[28] W. Hess, Macromolecules **21**, 2620 (1988).

[29] D. Richter, B. Ewen, B. Farago, and T. Wagner, Phys. Rev. Lett. **62**, 2140 (1989).

[30] D. Richter *et al.*, Macromolecules **25**, 6156 (1992).

[31] D. Richter *et al.*, Phys. Rev. Lett. **71**, 4158 (1993).

[32] B. Dünweg and K. Kremer, J. Chem. Phys. **99**, 6983 (1993).

[33] J. P. Hansen and I. R. McDonald, *Theory of Simple Liquids* (Academic Press, London, 1986).

[34] P. E. Rouse, J. Chem. Phys. **21**, 1272 (1953).

[35] P. H. Verdier, J. Chem. Phys. **27**, 2118 (1966).

[36] U. Ebert, A. Baumgärtner, and L. Schäfer, Phys. Rev. Lett. **78**, 1592 (1997).

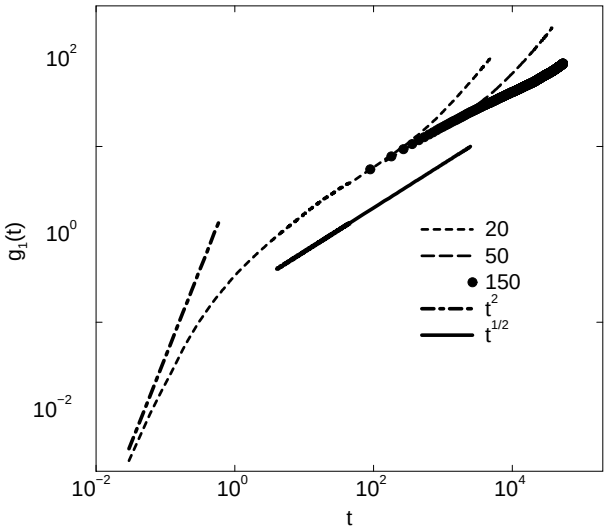

FIG. 1. Monomer displacement $g_1(t)$ of a pure system for various chain lengths as indicated in the figure. As a guide to the eye the power laws t^2 for the short–time regime and $t^{0.5}$ for the intermediate regime are included.

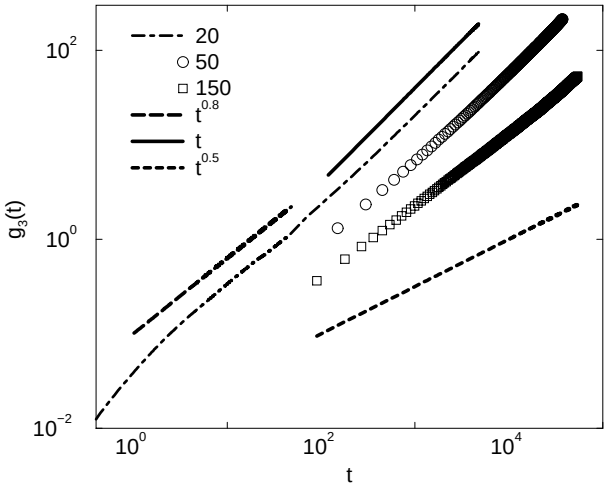

FIG. 2. Center–of–mass displacement $g_3(t)$ of a pure system for various chain lengths as indicated in the figure. The power laws $t^{0.8}$, $t^{0.5}$ and t^1 are shown as guide to the eye.

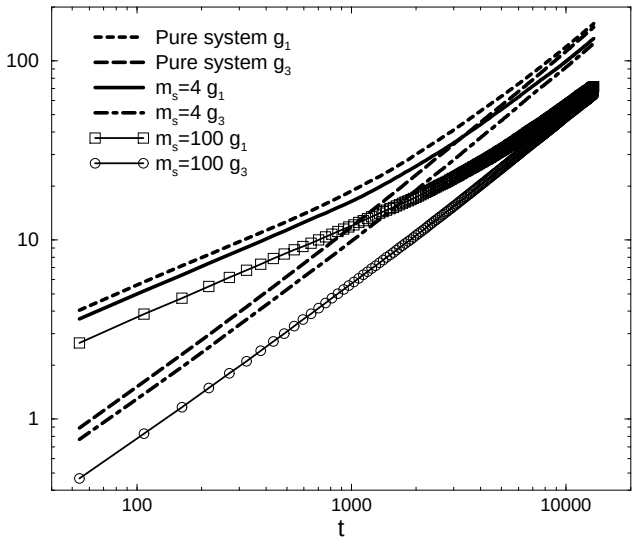

FIG. 3. Displacements g_1 and g_3 of the light chains ($m = m_f = 1$) in a pure system and two 50% mixtures with varying heavy mass ($m_s/m_f = 4, 100$). The chain length is $N = 30$.

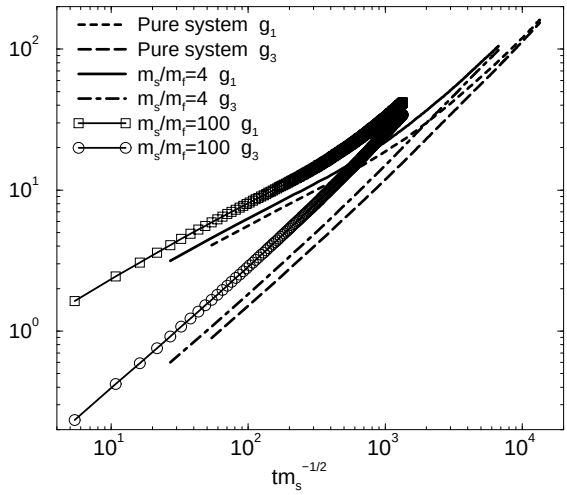

FIG. 4. Displacements g_1 and g_3 of the heavy chains as a function of scaled time $tm_s^{-1/2}$ in a pure system and two 50% mixtures with varying heavy mass ($m_s/m_f = 4,\ 100$). The chain length is $N = 30$.

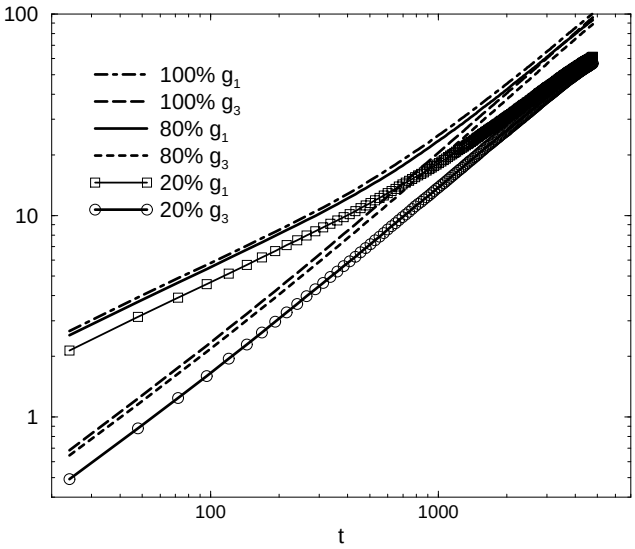

FIG. 5. Displacements g_1, g_3 of the light chains $m = m_f = 1$ for mixtures with a mass ratio of $m_s/m_f = 4$ and chain length $N = 20$. Data for various mixing ratios are shown, as indicated in the figure.

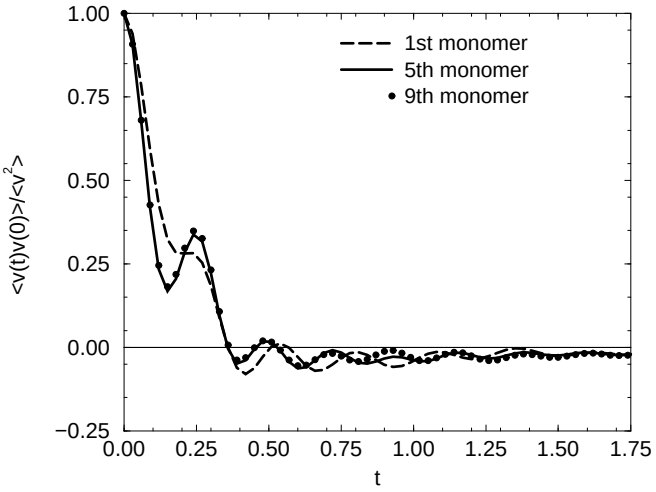

FIG. 6. Velocity autocorrelation function of the first, fifth and ninth monomer in a pure system with $m = 4$ and $N = 20$.

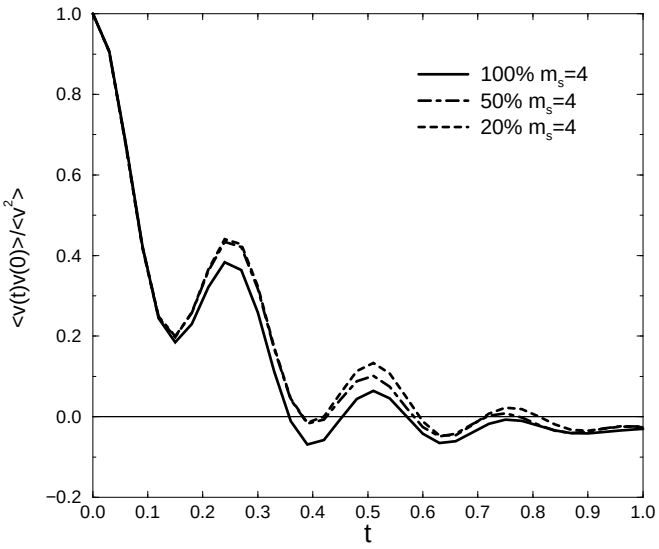

FIG. 7. Velocity autocorrelation function of a middle monomer of the heavy species for systems of chain length $N = 20$ and fixed mass ratio $m_s/m_f = 4$. The fractions indicated in the figure refer to the fraction of *heavy* chains.

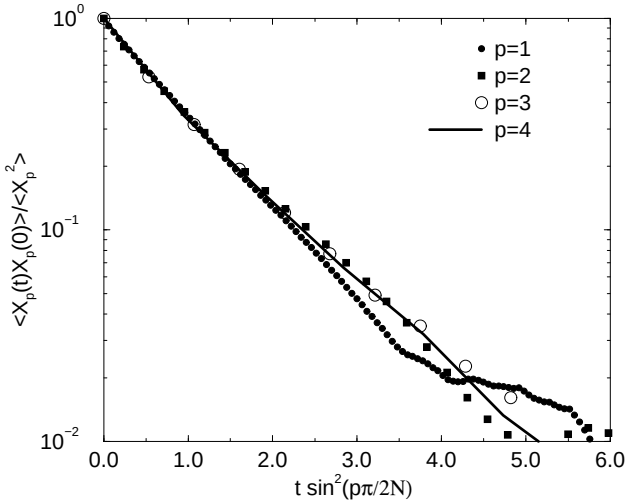

FIG. 8. Normalized autocorrelation function of the first four modes of a pure system ($m = 1$, $N = 30$) plotted against scaled time.

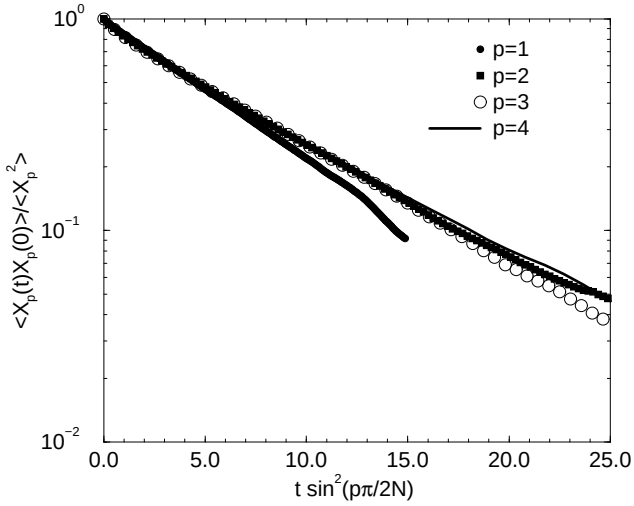

FIG. 9. Normalized mode autocorrelation function of the heavy chains as a function of scaled time for a mixture with $m_s/m_f = 100$, 20% light chains, and chain length $N = 30$.

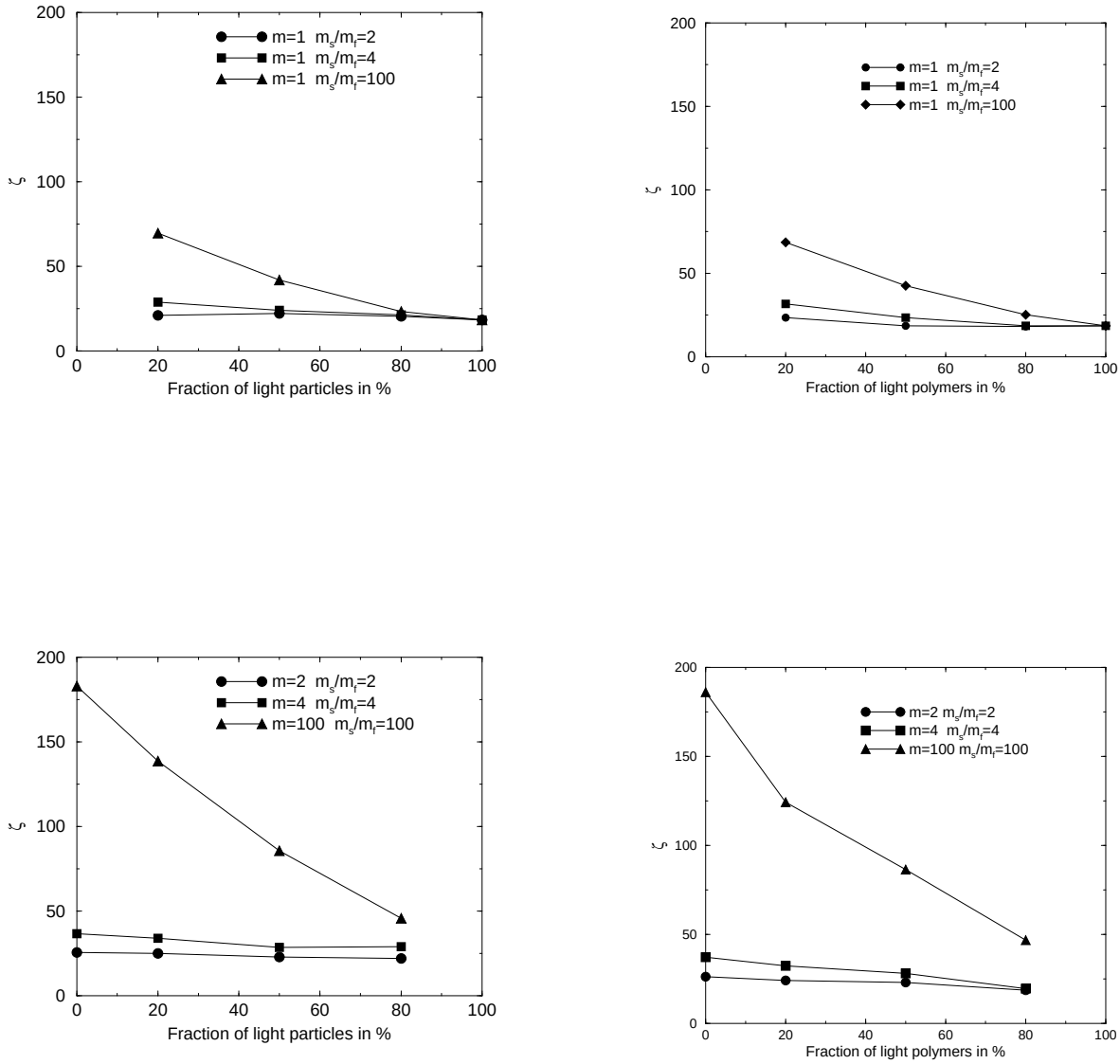

FIG. 10. Monomer friction coefficient of the light polymer species (upper part) and of the heavy species (lower part) as a function of composition. Data for $N = 20$ are shown in the left half of the figure and data for $N = 30$ in the right part.

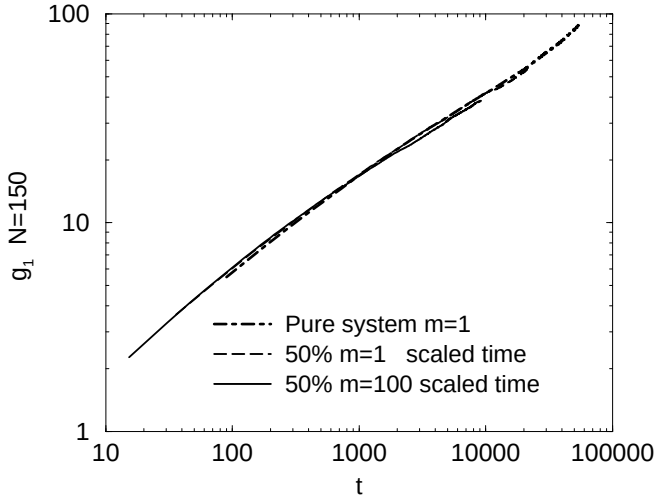

FIG. 11. Mean square displacement g_1 for systems with chain length $N = 150$. Data for a pure system as well as for a 50% mixture (both heavy and light chains) are included as indicated in the figure. For the data sets of the mixed systems, time was rescaled in order to superimpose the data on top of each other.

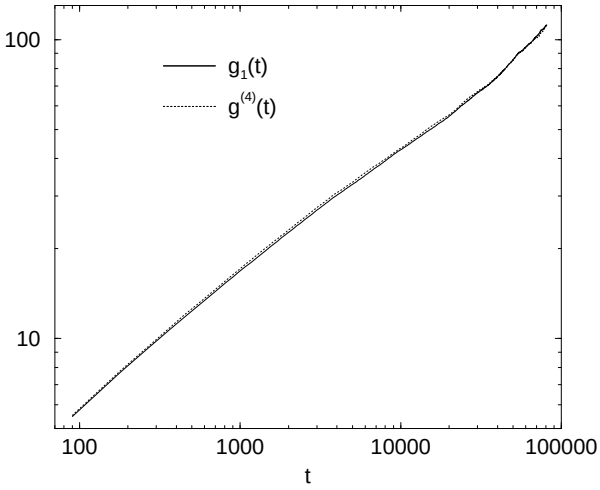

FIG. 12. $g_1(t)$ and $g^{(4)}(t)$ (see text) for a pure system with chain length $N = 150$.

TABLES

M	N	L	R^2	R_G^2	P	t	m_s/m_f	x
25	10	6.65	12.9	2.2	5.28	1×10^6	1, 2, 4	0, 20, 52, 80 %
30	20	8.90	29.5	4.9	5.15	4×10^6	1, 2, 4, 100	0, 20, 50, 80 %
20	30	8.90	46.1	7.6	5.00	9×10^6	1, 2, 4, 100	0, 20, 50, 80 %
16	50	9.80	80.5	13.3	4.95	25×10^6	1, 2, 4, 100	0, 18.75, 50, 81.25 %
20	75	12.08	123.8	20.4	4.93	56×10^6	1, 2, 4	0, 20, 50, 80 %
20	150	15.23	243.6	41.3	4.86	33×10^6	1, 100	0, 20, 50, 80 %

TABLE I. Simulation parameters and some quantities: M, number of chains in the system, N, degree of polymerization, L, length of the cubic box, R^2, mean square end–end distance, R_G^2, mean square gyration radius, P, pressure, t, length of run (in MD steps), m_s/m_f, mass ratio, x, fraction of slow chains.

N	$\zeta(N, p=1)$	$\zeta(N, p=2)$	$\zeta(N, p=3)$	$\zeta(N, p=4)$
10	19.9	20.1	19.9	20.6
20	18.3	20.8	21.2	20.5
30	18.6	20.8	21.4	20.9

TABLE II. Data for the monomeric friction coefficient for different chain lengths N and mode indexes p for pure systems.

Figure Captions

1. Monomer displacement $g_1(t)$ of a pure system for various chain lengths as indicated in the figure. As a guide to the eye the power laws t^2 for the short–time regime and $t^{0.5}$ for the intermediate regime are included.

2. Center–of–mass displacement $g_3(t)$ of a pure system for various chain lengths as indicated in the figure. The power laws $t^{0.8}$, $t^{0.5}$ and t^1 are shown as guide to the eye.

3. Displacements g_1 and g_3 of the light chains ($m = m_f = 1$) in a pure system and two 50% mixtures with varying heavy mass ($m_s/m_f = 4, 100$). The chain length is $N = 30$.

4. Displacements g_1 and g_3 of the heavy chains as a function of scaled time $tm_s^{-1/2}$ in a pure system and two 50% mixtures with varying heavy mass ($m_s/m_f = 4$, 100). The chain length is $N = 30$.

5. Displacements g_1, g_3 of the light chains $m = m_f = 1$ for mixtures with a mass ratio of $m_s/m_f = 4$ and chain length $N = 20$. Data for various mixing ratios are shown, as indicated in the figure.

6. Velocity autocorrelation function of the first, fifth and ninth monomer in a pure system with $m = 4$ and $N = 20$.

7. Velocity autocorrelation function of a middle monomer of the heavy species for systems of chain length $N = 20$ and fixed mass ratio $m_s/m_f = 4$. The fractions indicated in the figure refer to the fraction of *heavy* chains.

8. Normalized autocorrelation function of the first four modes of a pure system ($m = 1$, $N = 30$) plotted against scaled time.

9. Normalized mode autocorrelation function of the heavy chains as a function of scaled time for a mixture with $m_s/m_f = 100$, 20% light chains, and chain length $N = 30$.

10. Monomer friction coefficient of the light polymer species (upper part) and of the heavy species (lower part) as a function of composition. Data for $N = 20$ are shown in the left half of the figure and data for $N = 30$ in the right part.

11. Mean square displacement g_1 for systems with chain length $N = 150$. Data for a pure system as well as for a 50% mixture (both heavy and light chains) are included as indicated in the figure. For the data sets of the mixed systems, time was rescaled in order to superimpose the data on top of each other.

12. $g_1(t)$ and $g^{(4)}(t)$ (see text) for a pure system with chain length $N = 150$.